

A Multi-Source Geospatial Framework for Quantifying Groundwater Recharge and Storage Change in Data-Scarce Arid Regions: Application to the Mandera Sub-Basin, Northern Kenya

Margaret Njoroge*, Mercy Mwaniki

Department of Geomatic Engineering and Geospatial Information Systems, Jomo Kenyatta University of Agriculture and Technology, Nairobi, Kenya

Email: *nmargaret536@gmail.com, mmwaniki@jkuat.ac.ke

How to cite this paper: Njoroge, M. and Mwaniki, M. (2026) A Multi-Source Geospatial Framework for Quantifying Groundwater Recharge and Storage Change in Data-Scarce Arid Regions: Application to the Mandera Sub-Basin, Northern Kenya. *Computational Water, Energy, and Environmental Engineering*, 15, 53-72. <https://doi.org/10.4236/cweee.2026.152004>

Received: March 18, 2026

Accepted: April 24, 2026

Published: April 27, 2026

Copyright © 2026 by author(s) and Scientific Research Publishing Inc.

This work is licensed under the Creative Commons Attribution International License (CC BY 4.0).

<http://creativecommons.org/licenses/by/4.0/>



Open Access

Abstract

Groundwater is the primary water source in arid and semi-arid regions, but its assessment is often hindered by limited observational data. This study presents a comprehensive geospatial framework to estimate groundwater recharge, changes in storage, and available resources in the Mandera sub-basin in northeastern Kenya. The framework combines GIS-based recharge calculations and GRACE/GRACE-FO mascon data (JPL RL06) satellite-derived groundwater storage estimates. Recharge was estimated using an inverse water-balance approach, combining effective rainfall from CHIRPS precipitation and FAO Penman-Monteith evapotranspiration with hydrogeological factors, including lithology, soil texture, and slope. Results show significant spatial variability: high recharge occurs in the southern and eastern sub-basins, where coarse, permeable sediments are present, while the northern and western regions, with shale and dolomite formations, exhibit low recharge. GRACE-derived groundwater storage anomalies indicate interannual variability across the Mandera sub-basin, with interannual variability driven by episodic rainfall events. Although Mann-Kendall trend analysis reveals a weak positive trend ($\tau = 0.134$, $p = 0.398$), it is not statistically significant and likely reflects short-term climatic variability rather than long-term aquifer recovery. The study demonstrates that integrating GIS-based recharge modeling with satellite observations provides a dependable, transferable framework for assessing groundwater variability in data-scarce arid regions, supporting evidence-based water

management and planning.

Keywords

Groundwater Recharge, GRACE/GRACE-FO Mascon Data (JPL RL06), Groundwater Storage Anomalies, GIS, Arid and Semi-Arid Regions, Mandera Basin

1. Introduction

Groundwater is the primary freshwater resource in Arid and Semi-Arid Lands (ASALs), where surface water is limited, episodic, or absent. In these regions, groundwater sustainability depends on the balance between highly variable recharge processes and increasing extraction driven by population growth, livestock needs, and climate variability [1] [2]. Throughout Sub-Saharan Africa, groundwater provides a significant portion of domestic and livestock water needs and is vital for drought resilience and long-term water security [3] [4]. Despite this dependence, quantitative assessments of groundwater recharge, storage dynamics, and sustainable yield are limited in many ASAL areas due to sparse monitoring networks and complex hydrogeologic conditions [5].

Kenya is classified as a water-scarce country, with renewable freshwater availability below 1000 m³ per capita. Water stress is most severe in northeastern Kenya, where recurrent droughts, high potential evapotranspiration, and the lack of perennial surface water systems make groundwater the main reliable water source. In Mandera County, borehole failures and increasing abstraction demand have risen during recent droughts, signaling growing pressure on local aquifer systems [6]. However, groundwater resources in the Mandera sub-basin have not been systematically assessed at the basin level, and existing evaluations mainly depend on point-based borehole data [7].

Estimating groundwater recharge and storage in ASAL environments is methodologically difficult. Recharge primarily occurs through episodic rainfall events, focused infiltration along alluvial systems, and preferential flow pathways, leading to significant spatial variability [1] [8]. Conventional physically based groundwater models need extensive hydrogeological parameterization and long-term calibration data, which are often unavailable in data-scarce regions [9] [10]. As a result, alternative methods that combine spatially distributed surface data with indirect observations of subsurface changes are increasingly being used [6] [10].

Geographic Information Systems (GIS) offer an effective framework for integrating spatial datasets relevant to recharge estimation, including rainfall, evapotranspiration, geology, soil texture, land cover, and topography [10] [11]. Multi-criteria and water-balance-based GIS methods have been widely used in arid and semi-arid regions to estimate both relative and absolute recharge and to identify groundwater potential zones [12] [13]. While these methods enhance the spatial

understanding of recharge processes, they do not directly address groundwater storage dynamics.

Satellite gravimetry, particularly observations from the Gravity Recovery and Climate Experiment (GRACE) and GRACE Follow-On missions, provides an independent means of quantifying temporal changes in terrestrial water storage, including groundwater storage, at regional scales [14]-[16]. GRACE-derived groundwater storage anomalies have revealed significant depletion trends in overexploited aquifer systems worldwide. However, GRACE's relatively coarse spatial resolution requires integration with complementary datasets and modeling approaches to support sub-basin-scale groundwater assessments, particularly in hydrogeologically heterogeneous ASAL settings [6] [13].

Recent studies indicate that combining GIS-based recharge estimation with GRACE/GRACE-FO mascon-derived groundwater storage observations and abstraction data can improve groundwater assessments by jointly constraining recharge and storage changes, within a consistent analytical framework [6]. Such integrated approaches remain underapplied in African ASAL regions and are largely absent in northeastern Kenya, where hydrogeological data limitations and transboundary basin settings further complicate groundwater evaluation [6] [11].

This study addresses this gap by applying an integrated geospatial and remote sensing framework to assess groundwater recharge and storage variability in the Mandera sub-basin of northeastern Kenya. Rainfall-derived recharge is estimated using a GIS-based inverse hydrogeologic-balance approach that incorporates climatic, geological, and land-surface controls. Groundwater storage changes are estimated using GRACE/GRACE-FO mascon data (JPL RL06) satellite observations, corrected for soil moisture and surface water components, and converted to groundwater storage variations using representative specific-yield estimates [11] [14]. The results provide spatially explicit estimates of recharge and quantify long-term trends in groundwater storage, thereby providing a transferable methodological framework for groundwater assessment in data-scarce ASAL environments.

2. Materials and Methods

2.1. Study Area and Data Sources

The study was conducted in the Mandera sub-basin, located in northeastern Kenya within the Ethiopia-Kenya-Somalia (ENN) transboundary basin. The region is characterized by arid to semi-arid conditions, high potential evapotranspiration, episodic rainfall, and strong reliance on groundwater for domestic, livestock, and drought-resilient water supply.

All spatial and temporal datasets used in this study were obtained from publicly available sources. Precipitation data were derived from the Climate Hazards Group InfraRed Precipitation with Stations (CHIRPS) dataset (v2.0), which provides near-global rainfall estimates at 0.05° (~5 km) resolution [7]. Potential evapotranspiration data were sourced from the FAO CLIMWAT 2.0 database [3]. Monthly

combined GRACE and GRACE Follow-On (GRACE-FO) Release 06 mascon Total Water Storage Anomaly (TWSA) products were obtained from the NASA Jet Propulsion Laboratory (JPL) Tellus portal. Digital elevation data were obtained from the Shuttle Radar Topography Mission (SRTM) with a spatial resolution of 30 m. Soil texture data were gathered from SoilGrids, and land use/land cover data were obtained from publicly available global land cover products. Lithological information was compiled from regional geological maps and published hydrogeological reports [15]. All spatial analyses were conducted using ArcGIS Pro (version 3.x, Esri Inc.) (Figure 1).

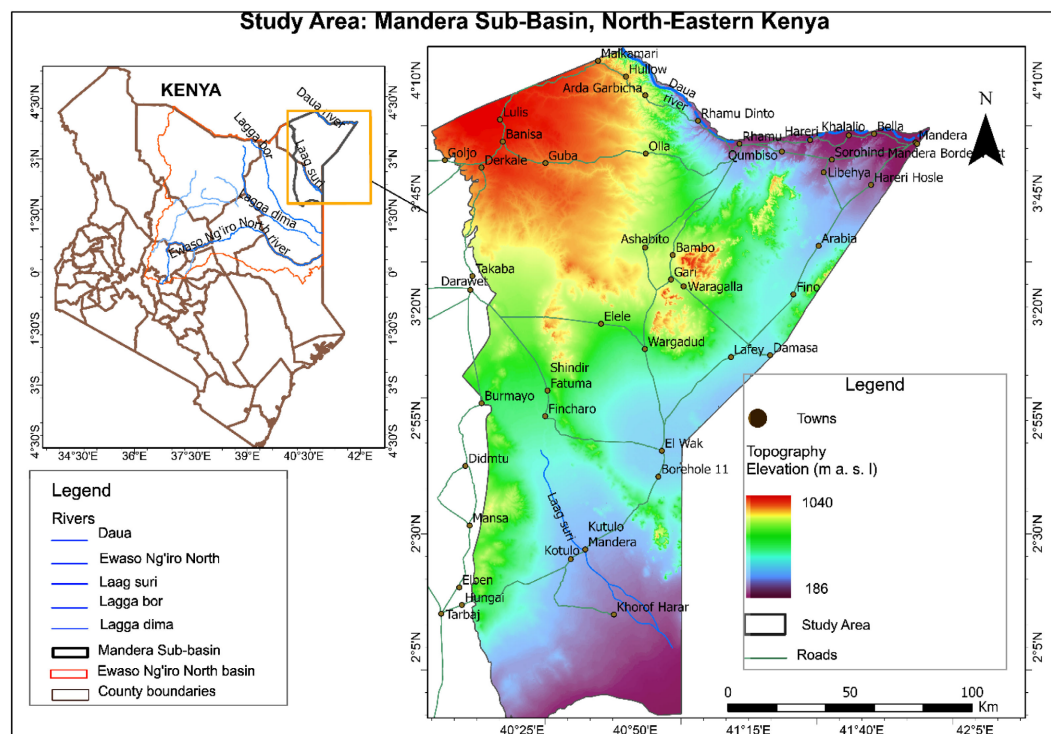


Figure 1. Location of the Mandera sub-basin in northeastern Kenya within the Ethiopia-Kenya-Somalia (ENN) transboundary basin.

2.2. Estimation of Groundwater Recharge

2.2.1. Conceptual Basis

Groundwater recharge in arid and semi-arid regions mainly happens through episodic high-intensity rainfall events, focused infiltration along temporary drainage systems, and preferential percolation through permeable lithological units and fracture networks [1]-[3]. In such environments, recharge varies greatly in space and time and is often driven by short, intense hydrological pulses rather than steady diffuse infiltration [2] [4]. Because long-term groundwater-level monitoring, tracer-based recharge measurements, and calibrated physically based groundwater-flow models are missing in the Mandera sub-basin, recharge was estimated using a spatially distributed hydrogeologic index approach based on climatic water-balance principles [5] [6]. Index-based and GIS-supported recharge estimation methods

are common in data-scarce arid and semi-arid regions, where direct recharge measurements are impractical [6]-[8].

The method combines effective rainfall with spatially variable infiltration controls based on lithology, soil texture, and slope, which are identified as the main factors influencing vertical percolation and groundwater recharge in sedimentary basins [2] [7] [9]. Unlike purely relative groundwater potential mapping methods, this framework provides quantitative recharge estimates ($\text{mm}\cdot\text{yr}^{-1}$ and $\text{m}^3\cdot\text{yr}^{-1}$) by integrating a climatic water-balance component with a dimensionless hydrogeologic transmissivity factor, scaled using conservative recharge coefficients that align with semi-arid basin studies [3] [5].

2.2.2. Estimation of Effective Rainfall

Mean annual precipitation (P) was derived from the Climate Hazards Group InfraRed Precipitation with Stations (CHIRPS) v2.0 dataset (0.05° spatial resolution) [7], which provides quasi-global rainfall estimates calibrated with station observations and is widely used in drought-prone African regions [1] [2]. Potential evapotranspiration (ET) was obtained from the FAO CLIMWAT 2.0 database, offering long-term climatic normals for water balance studies [3]. Effective rainfall (P_e), representing the portion of rainfall potentially available for groundwater recharge after atmospheric losses, was calculated using a water-balance method [4] [5], as shown in Equation (1).

$$P_e = P - ET \quad (1)$$

This formulation offers a conservative upper limit on evaporative losses, where potential evapotranspiration can surpass actual evapotranspiration in water-scarce arid environments [4] [5]. Effective rainfall values were limited to non-negative numbers to prevent artificial recharge deficits.

2.2.3. Hydrogeological Infiltration Index

A dimensionless hydrogeological factor (H) representing infiltration capacity in Equation (2) is calculated by a weighted linear combination of standardized thematic layers.

$$H = (w_1G) + (w_2S) + (w_3Sl) \quad (2)$$

where G represents lithology, S is soil texture, Sl is slope, and $w_1 - w_3$ are assigned infiltration weights. To ensure reproducibility and reduce subjectivity in the assignment of thematic weights, a rule-based weighting scheme was adopted based on the relative control of each factor on vertical percolation as documented in hydrogeological literature [6]. Lithology (G) and soil texture (S) were assigned higher weights (0.35 each) because they directly control permeability, porosity, and hydraulic conductivity, which govern infiltration and storage capacity. Slope (Sl) was assigned a slightly lower weight (0.30) as it primarily influences runoff generation and residence time rather than subsurface flow properties [4] [6].

Each thematic layer was classified into five ordinal infiltration-suitability classes (1 = very low to 5 = very high); lithology classes were ranked based on perme-

ability (e.g., shale = low, sand/gravel = high), soil texture based on grain size and infiltration capacity (e.g., clay = low, sandy soils = high), slope based on runoff potential (steep slopes = low infiltration, gentle slopes = high infiltration). The hydrogeological factor (H) was computed as a normalized weighted sum of these standardized classes, ensuring that all inputs contribute consistently and that H remains dimensionless and bounded between minimum and maximum suitability values, as shown in Equation (3) below:

$$\sum W_i = 1 \quad (3)$$

2.2.4. Recharge Calculation

Mean annual groundwater recharge (R) was calculated by combining effective rainfall with the hydrogeological factor.

$$R_d = \beta (P_e \times H) \quad (4)$$

where: R_d is the mean annual groundwater recharge (depth, usually in mm/yr or m/yr).

P_e is effective rainfall (portion of precipitation available for recharge after evapotranspiration losses).

H is the hydrogeological infiltration factor (dimensionless index representing the combined effects of lithology, soil texture, slope, and sometimes land cover).

β is an empirical scaling coefficient that adjusts the water-balance product ($P_e \times H$) to a realistic estimate of actual recharge.

In Equation (4), β is an empirical recharge efficiency coefficient (dimensionless) that represents the fraction of effective rainfall and hydrogeological potential that actually contributes to groundwater recharge. It accounts for losses due to evapotranspiration, surface runoff, and preferential flow processes not explicitly represented in the index model [4] [8].

Based on published recharge studies in semi-arid sedimentary basins, long-term recharge typically ranges from 2% to 15% of annual precipitation [4] [5] [10]. To maintain consistency with this range and avoid overestimation, β was constrained between 0.05 and 0.15, with a baseline value of 0.10 selected for the main analysis. This midpoint value represents a conservative estimate appropriate for arid environments where recharge is episodic and limited. This coefficient scaling helps prevent systematic overestimation of recharge that can occur with purely index-based methods [7] [8].

Raster map algebra was used to ensure pixel-level integration of all datasets. For each raster cell, the volumetric calculation was performed as shown in Equation (5) below:

$$V_c = R_d \times A_c \quad (5)$$

where V_c is the recharge volume per cell ($\text{m}^3 \cdot \text{yr}^{-1}$), R_d is the recharge depth ($\text{m} \cdot \text{yr}^{-1}$) and A_c is the cell area (m^2). Total basin recharge is calculated using Equation (6) by summing all cell volumes within the basin:

$$R_{basin} = \sum_{i=1}^n V_{c,i} \quad (6)$$

The recharge coefficient values (R/P) were compared with published recharge estimates from semi-arid East African basins to ensure physical plausibility [5] [11]. The resulting basin-average recharge fell within accepted semi-arid recharge ranges, reducing the likelihood of systematic bias.

2.3. GRACE-Based Groundwater Storage Analysis

2.3.1. GRACE and GLDAS Data Processing

Monthly combined GRACE and GRACE Follow-On (GRACE-FO) Release 06 mascon Total Water Storage Anomaly (TWSA) products were obtained from the NASA Jet Propulsion Laboratory (JPL) Tellus portal. The dataset provides a continuous time series from April 2002 to 2024, combining observations from the original GRACE mission (2002-2017) and the GRACE-FO mission (2018-present), with a short data gap between missions. The mascon solutions have an effective spatial resolution of approximately 0.5° (~ 55 km). JPL-provided scaling (gain) factors were applied to correct for signal attenuation and leakage effects inherent in GRACE/GRACE-FO mascon data (JPL RL06) processing [12] [14]. Soil moisture storage anomaly (SMSA), surface runoff (Q_s), and canopy water storage anomaly (CWSA) data were obtained from the Global Land Data Assimilation System (GLDAS) Noah model version 2.1 at 0.25° resolution [11]. These datasets were temporally aligned with GRACE observations.

GRACE/GRACE-FO mascon data were spatially aggregated to the Mandera sub-basin by applying an area-weighted averaging approach. The basin boundary was overlaid on the mascon grid, and for each time step, the basin-average Total Water Storage Anomaly (TWSA) was computed as the weighted mean of all intersecting mascon cells, with weights proportional to the fraction of each grid cell falling within the basin. This approach preserves the native resolution of the GRACE mascon data and avoids artificial spatial disaggregation. Groundwater Storage Anomalies (GWSA) were computed using the residual method by disaggregating GRACE/GRACE-FO TWSA into water storage components [12]

$$GWSA = TWSA - (SMSA + Q_s + CWSA) \quad (7)$$

All terms represent basin-averaged monthly anomalies expressed as equivalent water height. This formulation follows established GRACE-based groundwater assessment methods [17]. GRACE-derived anomalies (mm equivalent water height) were converted to volumetric groundwater storage change, calculated using Equation (8):

$$\Delta GWSA = \Delta h \times A \quad (8)$$

where: Δh = equivalent water height change (m), A = basin area (m^2).

The groundwater storage anomalies were also used to calculate the volumetric groundwater storage change by scaling the equivalent water height by the sub-basin area. Groundwater level changes (Δh) were estimated using representative aquifer-specific yield values (S_y):

$$\Delta h = \frac{\text{GWSA}}{S_y} \quad (9)$$

Specific yield (S_y) values were selected based on commonly reported properties of sedimentary aquifers, with unconsolidated sands typically exhibiting higher drainable porosity than fractured sandstones. Representative ranges include unconsolidated sands ($S_y \approx 0.15 - 0.25$) and fractured sandstones ($S_y \approx 0.05 - 0.15$), consistent with published hydrogeological compilations of specific yield for different lithologies [11]. For the basin-scale approximation, a representative value of $S_y = 0.15$ based on regional hydrogeological studies of unconsolidated sedimentary aquifers in northeastern Kenya [11] was used to convert equivalent water-height changes into an approximate water-table decline. This conversion primarily reflects unconfined aquifer behavior; confined aquifer storage changes are governed by storativity rather than specific yield and may not translate directly to water-table decline [11].

2.3.2. Trend Analysis of Groundwater Storage

Long-term trends in groundwater storage anomalies were evaluated using the Mann-Kendall test, a nonparametric method widely used for detecting monotonic trends in hydrological time series [15]. To reduce short-term variability and serial correlation inherent in monthly GRACE/GRACE-FO data, the groundwater storage anomaly time series was aggregated to annual averages for the period 2003-2024, resulting in $n = 22$ observations. The Mann-Kendall test was then applied to this annual time series. The test does not require the data to follow a normal distribution and is robust to missing values and outliers, making it suitable for satellite-derived groundwater datasets.

The Mann-Kendall statistic (τ) was computed for the monthly Groundwater Storage Anomaly (GWSA) time series to determine whether a statistically significant increasing or decreasing trend exists over the study period. The magnitude of the detected trend was estimated using Sen's slope estimator, which computes the median rate of change across all pairs of observations in the time series [16]. Sen's slope provides a robust estimate of the annual groundwater storage change expressed in millimeters per year ($\text{mm}\cdot\text{yr}^{-1}$) of equivalent water height. The combined application of the Mann-Kendall test and Sen's slope estimator provides both the statistical significance and magnitude of groundwater storage trends, allowing assessment of long-term aquifer depletion within the Mandera sub-basin.

3. Results

3.1. Groundwater Recharge Estimation

Applying the climatic water-balance formulation (Equation (1)) produced basin-wide estimates of effective rainfall (P_e), which represents the portion of precipitation potentially available for groundwater recharge after atmospheric losses. The analysis shows that only a small part of annual precipitation contributes to possible recharge due to high evaporative demand typical of semi-arid climates. Poten-

tial evapotranspiration greatly offsets precipitation across most of the Mandera sub-basin, limiting the amount of effective rainfall available for infiltration. As a result, effective rainfall varies significantly across the basin, influenced by local precipitation patterns and evapotranspiration gradients. Areas in the southern and eastern parts of the basin, with relatively higher rainfall and lower evaporative losses, have higher effective rainfall than the northern and western regions. The spatial distribution of effective rainfall across the basin is shown in **Figure 2**.

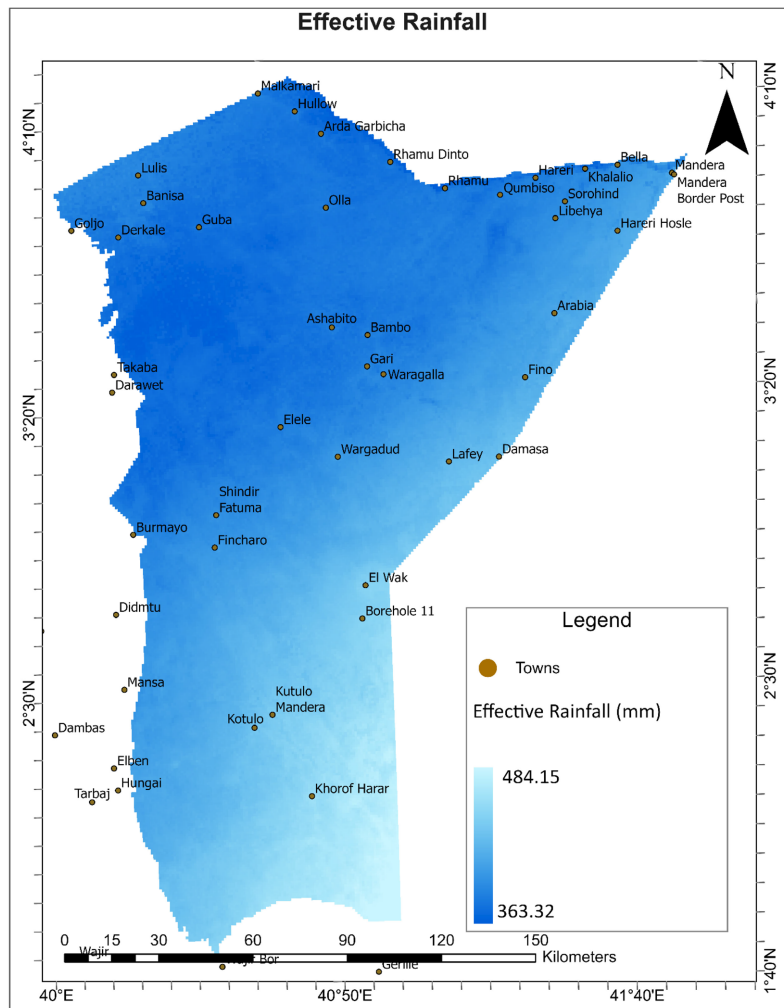


Figure 2. Spatial distribution of effective rainfall derived from mean annual precipitation and evapotranspiration.

3.2. Hydrogeological Controls and Spatial Distribution of Groundwater Recharge

The hydrogeological infiltration index (H), calculated using Equation (2), combines lithology, soil texture, and slope to depict the spatial variability of infiltration capacity across the Mandera sub-basin. Lithology and soil texture have the strongest effect on infiltration because they control permeability and hydraulic conduc-

tivity, while slope influences the partition between surface runoff and infiltration by regulating the duration that rainfall remains on the land surface.

Combining effective rainfall with the hydrogeological infiltration index produced spatially distributed estimates of groundwater recharge across the basin. The analysis indicates that recharge is highest in the southern and eastern sectors, where permeable sediments and favorable infiltration conditions prevail. In contrast, northern and western areas show limited recharge due to low-permeability lithological formations. The spatial distribution of estimated groundwater recharge is presented in **Figure 3**.

Comparing recharge distribution with existing groundwater abstraction points reveals a spatial mismatch between borehole locations and areas with high recharge potential. Several boreholes are located in zones characterized by low recharge capacity, which may contribute to localized groundwater stress. The relationship between recharge zones and borehole locations is illustrated in **Figure 4** (**Table 1**).

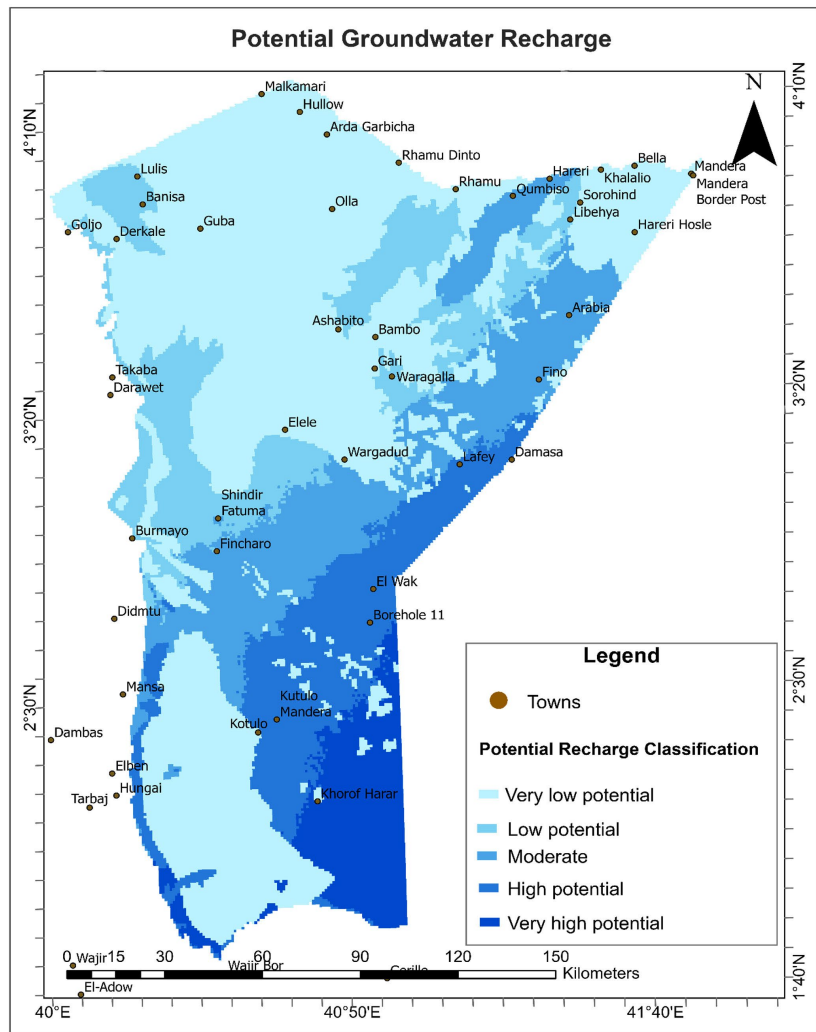


Figure 3. Spatial distribution of estimated groundwater recharge in the Mandera sub-basin.

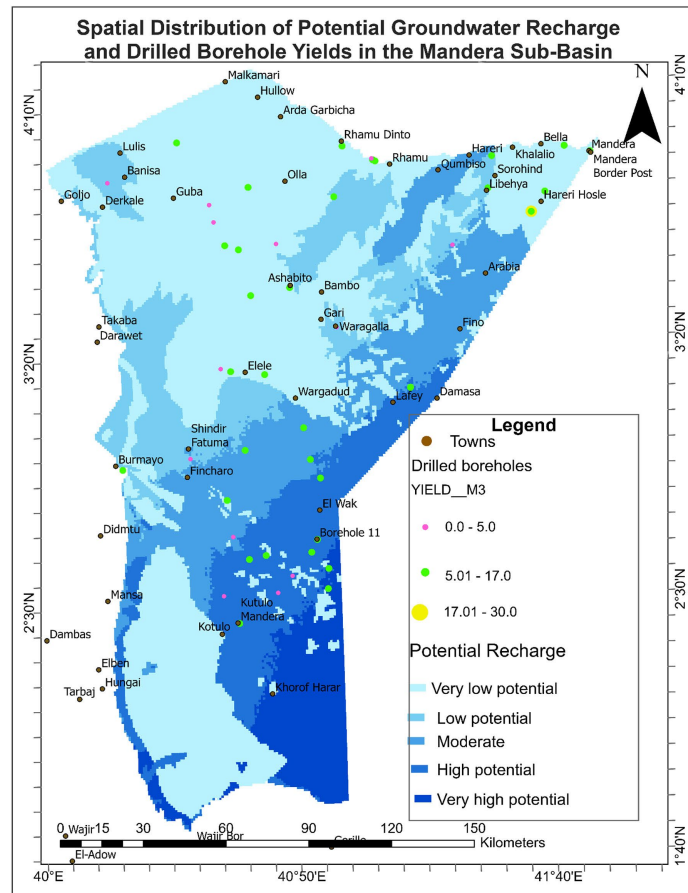


Figure 4. Relationship between estimated groundwater recharge zones and borehole locations in the Mandera sub-basin, highlighting areas where groundwater abstraction points occur relative to recharge potential.

Table 1. Hydrogeological recharge zones in the Mandera sub-basin.

Recharge Zone	Borehole Distribution (%)	Dominant Lithology	Representative Formations/Units	Hydrogeological Characteristics
Very Low Recharge Zone	38.7%	Dolomites, shales, fine-grained sandstones	Bajocian-Upper Jurassic (Posidonia Shales, Kambe Oolitic Limestone—J2; J3 Shales; Tithonian-Neocomian Mandera Series)	Low permeability; confined to semi-confined aquifers; localized recharge along riverbanks (Daua & Laah Boor)
Low Recharge Zone	19.35%	Colluvial sands, interbedded shale-limestone sequences	Marginal Bajocian-Upper Jurassic units and colluvial deposits	Limited infiltration; recharge via fractures and ephemeral runoff
Moderate Recharge Zone	29.03%	Pebble sheets, red soils, and old surface formations	Holocene continental sediments (Garissa area)	Moderate transmissivity; secondary porosity; diffuse infiltration
High Recharge Zone	12.9%	Coarse sands and gravels	Elwak Sands (Pleistocene, Quaternary sediments)	High permeability; unconfined aquifers; direct recharge from rainfall and stream infiltration

3.3. Groundwater Storage Dynamics from GRACE Observations

3.3.1. Groundwater Storage Anomalies

Groundwater storage anomalies were derived from the combined GRACE/GRACE-FO mascon time series (2003-2024), ensuring continuity across both satellite missions. Analysis of GRACE-derived Total Water Storage Anomalies shows substantial interannual variability, with a weak and statistically non-significant long-term trend (Figure 5). From 2003 to 2024, groundwater storage has exhibited a persistent downward trend, with partial rebounds during periods of above-average rainfall, such as in 2018. Although GRACE/GRACE-FO data provide basin-scale averages, comparison with spatial patterns of abstraction and recharge suggests that observed storage declines are likely influenced by areas of higher groundwater use, particularly in the southern and central parts of the basin.

Groundwater Storage Anomalies (GWSA), derived using the residual water-balance method (Equation (7)), further confirm this trend. Observed GWSA values range between -0.40 m and -0.63 m of equivalent water height, indicating ongoing basin-wide groundwater depletion throughout the observation period. The spatial pattern of groundwater storage anomalies is presented in Figure 6, and the temporal evolution of TWSA during the study period is shown in Figure 5.

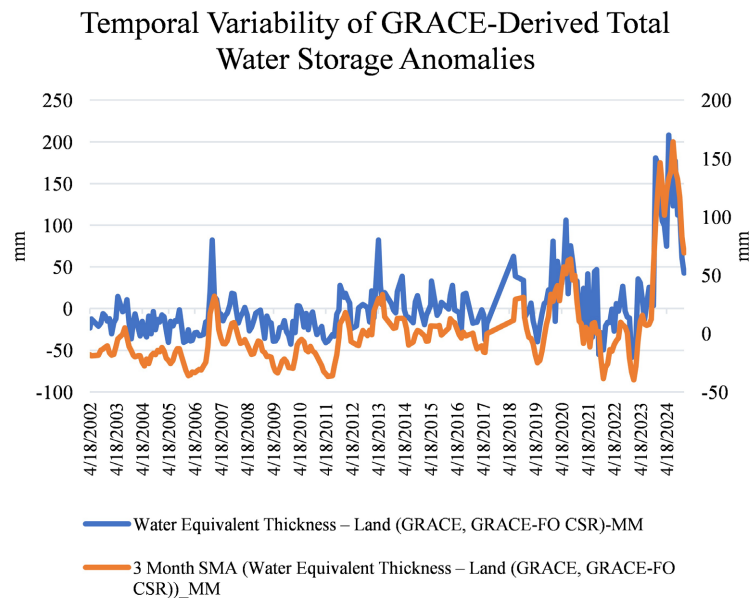


Figure 5. Temporal variability of GRACE-derived Total Water Storage Anomalies (TWSA) in the Mandera sub-basin from 2003-2024, showing multi-year fluctuations associated with climatic variability.

3.3.2. Trend Analysis Using the Mann-Kendall Test

The Mann-Kendall trend analysis was performed on the annual groundwater storage anomaly time series ($n = 22$) derived from aggregated monthly GRACE/GRACE-FO data. The results indicate a weak positive trend in groundwater storage anomalies over the study period. The Mann-Kendall test produced a statistic of $S = 31$ with Kendall's tau (τ) = 0.134, suggesting a slight upward tendency in groundwa-

ter storage anomalies. The standardized test statistic ($Z = 0.85$) corresponds to a p-value of approximately 0.40, which is greater than the significance threshold of 0.05. This indicates that the detected trend is not statistically significant at the 95% confidence level.

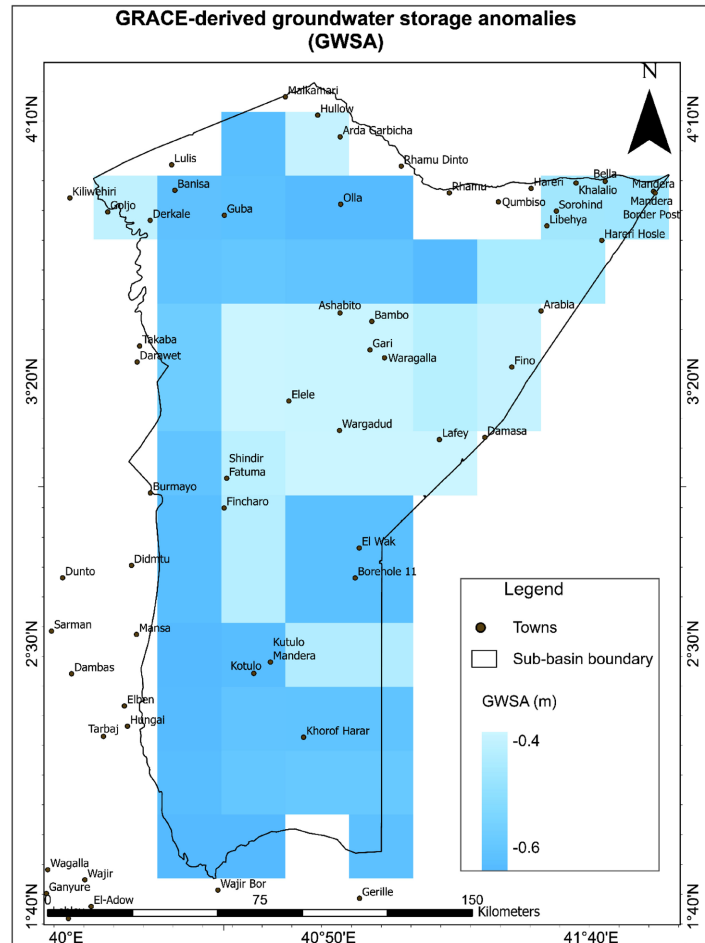


Figure 6. Basin-averaged groundwater storage anomalies derived from GRACE/GRACE-FO mascon data (coarse spatial resolution).

The magnitude of the trend estimated using Sen's slope was 1.12 mm per year, indicating a slight increase in groundwater storage anomalies during the study period. However, given the lack of statistical significance, the observed increase may reflect natural interannual variability rather than a persistent long-term trend.

Table 2. Mann-Kendall trend test and Sen's slope results for GRACE/GRACE-FO-derived groundwater storage anomalies in Mandera County (2003-2024).

Parameter	Value
Number of observations (n)	22
Mann-Kendall S statistic	31
Kendall's tau (τ)	0.134

Continued

Z statistic	0.85
p-value	0.398
Sen's slope	1.12 mm/year
Trend direction	Increasing
Statistical significance ($\alpha = 0.05$)	Not significant

The statistical results confirm a weak upward trend in groundwater storage anomalies, although it is not statistically significant at the 95% confidence level (Table 2).

The observations indicate episodic declines in groundwater storage associated with drought periods; however, the Mann-Kendall analysis does not show a statistically significant long-term trend.

3.3.3. Estimated Water Table Decline

Groundwater Storage Anomalies (GWSA) were converted into equivalent groundwater-level changes using a typical specific yield value of $S_y = 0.15$ (Equation (9)). This conversion provides an approximate measure of water-table fluctuations associated with observed storage changes during the study period. The results show that groundwater levels across the Mander sub-basin dropped by approximately -1.84 m to -2.87 m. The spatial distribution of the estimated water-table changes generally reflects the pattern seen in the GWSA results, indicating a consistent link between regional groundwater storage depletion and groundwater-level decline.

The most significant drawdowns occur in the southern and midwestern regions of the basin, where groundwater extraction is more intensive, and recharge conditions are relatively limited. In contrast, smaller declines are seen in the basin's northern and eastern areas. These spatial patterns show localized zones of increased groundwater stress that may be linked to concentrated pumping for domestic use, livestock watering, and small-scale irrigation (Figure 7).

3.3.4. Sensitivity Analysis of Recharge Estimates

To evaluate the sensitivity of recharge estimates to key assumptions, a simple uncertainty analysis was conducted by varying the empirical recharge coefficient (β) and specific yield (S_y) within plausible ranges reported for semi-arid sedimentary aquifers [17]. Recharge was recalculated using β values of 0.05 (lower bound), 0.10 (baseline), and 0.15 (upper bound). The results indicate that basin-average recharge varies proportionally with β , producing an estimated range of approximately:

- Lower bound ($\beta = 0.05$): ~ 0.9 mm \cdot yr $^{-1}$.
- Baseline ($\beta = 0.10$): ~ 1.8 mm \cdot yr $^{-1}$.
- Upper bound ($\beta = 0.15$): ~ 2.7 mm \cdot yr $^{-1}$.

This range demonstrates that recharge estimates are moderately sensitive to the choice of β , though all values remain within typical semi-arid recharge limits. Sim-

ilarly, groundwater-level change estimates derived from GRACE/GRACE-FO mascon data (JPL RL06) were evaluated using a range of specific yield values ($S_y = 0.05 - 0.25$), reflecting variability between fractured and unconsolidated sedimentary aquifers. The resulting estimated groundwater-level decline ranges from approximately (Table 3):

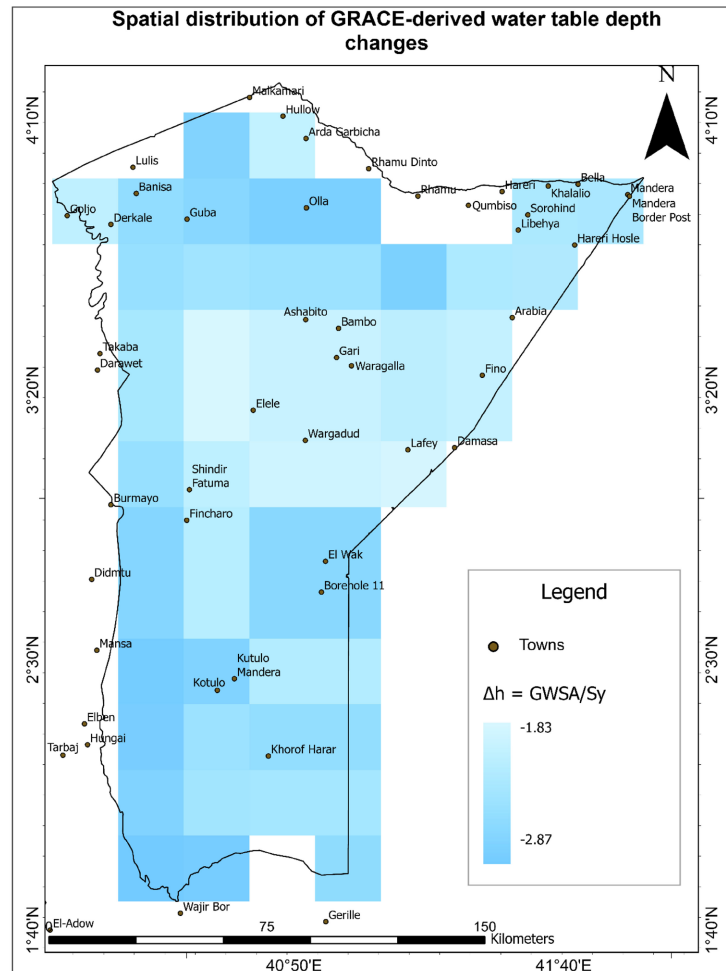


Figure 7. Spatial distribution of estimated groundwater-level changes across the Mandera sub-basin derived from groundwater storage anomalies (GWSA) using a representative specific yield of $S_y = 0.15$.

- $S_y = 0.25 \rightarrow$ smaller decline ($\sim 1.1 - 1.7$ m).
- $S_y = 0.15 \rightarrow$ baseline ($\sim 1.8 - 2.9$ m).
- $S_y = 0.05 \rightarrow$ larger decline ($\sim 5 - 8$ m).

These results indicate that groundwater-level estimates are highly sensitive to assumptions about specific yield, highlighting the importance of constraining aquifer properties where possible. The sensitivity analysis indicates that uncertainty in β and specific yield can significantly influence recharge and groundwater-level estimates; however, the adopted parameter ranges ensure that results remain within physically realistic bounds for semi-arid sedimentary basins.

Table 3. Summary of groundwater characteristics and trends across the Mandera sub-basin.

Parameter	Observed Range/Value	Spatial Pattern	Interpretation
Recharge (mm/yr)	~18 mm/yr	Higher in the southern sector, moderate in the east, and lower in the northern parts of the basin	Recharge distribution is primarily controlled by lithology, topography, and infiltration conditions
Groundwater Storage Anomaly (GWSA) (mm)	Sen's slope = 1.12 mm/yr	Basin-wide variability with localized fluctuations Statistical trend Mann-Kendall: $S = 31$, $\tau = 0.134$, $p = 0.398$ (not significant)	Weak increasing tendency in groundwater storage anomalies; trend not statistically significant, suggesting largely stable storage with interannual variability
Water Table Change (m)	-1.84 to -2.87	Decline corresponds with areas of higher groundwater use and recharge variability	Declining water levels indicate localized aquifer stress, likely associated with abstraction and climatic variability

4. Discussions

The results demonstrate that groundwater recharge in the Mandera sub-basin is highly spatially heterogeneous and primarily controlled by lithology, soil texture, and slope. Southern and eastern sectors, dominated by coarse sands and Quaternary sediments, exhibit higher infiltration and recharge due to favorable hydraulic conductivity, porosity, and gentle slopes. In contrast, the northern and western regions, underlain by Jurassic shales and dolomitic formations, display limited recharge potential, as low-permeability units promote runoff and restrict vertical percolation. Recharge is largely episodic, occurring during intense rainfall events and along ephemeral drainage systems such as the Daua River. These findings confirm that the sub-basin operates under a recharge-limited regime and are consistent with observed spatial patterns of effective rainfall and hydrogeological suitability, which have been widely documented in arid and semi-arid aquifer systems across Africa [1] [2].

GRACE/GRACE-FO satellite analysis indicates a multi-decadal decline in groundwater storage anomalies ranging from -0.40 m to -0.63 m across the basin. These results correspond with estimated groundwater-level declines of approximately -1.84 m to -2.87 m. The decline correlates with prolonged droughts between 2009 and 2015. Despite this decline, the degree of depletion varies spatially, indicating localized stress rather than uniform basin-wide groundwater exhaustion. Mann-Kendall trend analysis indicates a weak, statistically non-significant upward trend ($\tau = 0.134$, $p = 0.398$), likely reflecting interannual climatic variability rather than sustained aquifer recovery. Similar patterns of climate-driven groundwater variability have been observed in several African aquifers where episodic recharge events dominate long-term storage dynamics [17]. The spatial variability in recharge and localized groundwater depletion highlights the importance of evidence-based groundwater management strategies that account for hydrogeological heterogeneity. Mapping high-recharge zones can help identify priority monitoring well locations and potential sites for recharge enhancement, while GRACE/GRACE-FO-derived Groundwater Storage Anomaly (GWSA) observations provide an early

indication of long-term aquifer stress.

The groundwater storage patterns observed in the Mandera sub-basin are broadly consistent with GRACE-based groundwater studies conducted in other arid and semi-arid regions of Africa. For example, GRACE satellite analyses in the Sahel region have shown that groundwater systems often exhibit strong interannual variability driven by episodic rainfall and multi-year drought cycles rather than consistent long-term monotonic trends [18]. Similar findings have been reported for the Niger Basin, where GRACE-derived terrestrial water storage anomalies reveal alternating periods of depletion and recovery associated with climatic variability and land-use changes [5]. In the East African Rift System, satellite-based gravimetry studies have also documented spatially heterogeneous groundwater responses, with localized abstraction and hydrogeological controls leading to uneven storage changes across basins [6]. Compared with these regional studies, the Mandera sub-basin shows a comparable pattern of moderate storage decline combined with short-term climatic variability, reinforcing the interpretation that groundwater dynamics in arid African basins are primarily governed by episodic recharge events, hydrogeological heterogeneity, and localized abstraction pressures.

The spatial distribution of boreholes relative to recharge zones shows a significant mismatch between groundwater abstraction points and areas with high recharge potential. This indicates that water scarcity in parts of the Mandera sub-basin may be more affected by poor borehole siting and infrastructure layout than by actual groundwater resource limits.

5. Study Limitations

While the integrated framework provides useful insights into groundwater dynamics in the Mandera sub-basin, several limitations should be acknowledged. First, the effective spatial resolution of GRACE/GRACE-FO satellite data is relatively coarse compared with the scale of local aquifer systems, potentially smoothing localized groundwater variations. Therefore, the resulting groundwater storage anomalies represent basin-scale averages and do not resolve local-scale variability within the sub-basin. Therefore, all interpretations of groundwater storage change are limited to regional trends rather than site-specific conditions. Second, the residual approach used to estimate groundwater storage anomalies relies on GLDAS model outputs for soil moisture and surface water components, which introduce additional uncertainty into the groundwater estimates. Despite these limitations, GRACE/GRACE-FO mascon observations provide one of the few reliable means of monitoring regional groundwater storage changes in data-scarce regions, and when combined with GIS-based recharge modeling, they offer a valuable tool for supporting groundwater assessment and management in arid and semi-arid environments.

6. Conclusions

This study developed and applied an integrated geospatial framework to assess

groundwater recharge, storage dynamics, and resource sustainability in the Mandera sub-basin of northeastern Kenya. The approach combines GIS-based recharge modeling, satellite gravimetry from GRACE and GRACE Follow-On missions, and hydrogeological analysis to evaluate groundwater conditions in a data-scarce arid environment.

The results indicate that groundwater recharge in the Mandera sub-basin is spatially heterogeneous and generally low, with an estimated basin-average recharge of approximately 1.8 mm yr^{-1} . Recharge is highest in the southern and eastern sectors of the basin, where permeable Quaternary sediments, gentle slopes, and relatively higher rainfall promote infiltration. In contrast, northern and western areas dominated by shale and dolomitic formations exhibit limited recharge due to low permeability and higher runoff potential. These findings confirm that groundwater replenishment in the basin is largely episodic and strongly controlled by hydrogeological conditions.

Analysis of the groundwater storage anomalies shows substantial interannual variability associated with climatic fluctuations, particularly drought periods and episodic rainfall events. Although the time series indicates localized groundwater depletion and estimated water-table declines of approximately 1.8 - 2.9 m in some parts of the basin, Mann-Kendall trend analysis reveals only a weak and statistically non-significant long-term trend in groundwater storage.

From a management perspective, the results highlight a spatial mismatch between existing borehole locations and areas with higher recharge potential. This suggests that groundwater stress in parts of the basin may be influenced more by borehole siting and infrastructure distribution than by absolute groundwater scarcity. The integrated framework presented in this study demonstrates the value of combining remote sensing and geospatial analysis for groundwater assessment in data-limited arid regions and can support evidence-based planning, monitoring, and sustainable groundwater management across similar ASAL environments.

Future research should focus on improving the temporal and spatial resolution of groundwater monitoring to complement GRACE satellite observations. Integrating high-resolution local data from observation wells, soil moisture sensors, and streamflow measurements would refine recharge estimates and reduce uncertainties in storage dynamics. Climate variability and projected changes in rainfall patterns should be incorporated into assessments of the potential impacts of droughts and extreme events on groundwater sustainability.

Data Availability

All datasets used in this study are publicly available from CHIRPS, NASA GRACE Tellus, GLDAS, and SoilGrids repositories.

Acknowledgements

The authors would like to acknowledge the institutions and data providers whose publicly available datasets made this research possible. Precipitation data were ob-

tained from the Climate Hazards Group InfraRed Precipitation with Stations (CHIRPS) dataset, while groundwater storage observations were derived from the GRACE and GRACE Follow-On missions provided by the NASA Jet Propulsion Laboratory (JPL) Tellus program. Soil moisture and related hydrological variables were obtained from the Global Land Data Assimilation System (GLDAS).

The authors are grateful to colleagues and reviewers whose comments and suggestions helped improve the clarity and quality of the manuscript.

The authors also acknowledge the Department of Geomatic Engineering and Geospatial Information Systems at Jomo Kenyatta University of Agriculture and Technology for academic support during this research.

Funding

This research received no external funding.

Conflicts of Interest

The authors declare that they have no known competing financial interests or personal relationships that could have influenced the work reported in this paper.

References

- [1] Taylor, R.G., Scanlon, B., Döll, P., Rodell, M., van Beek, R., Wada, Y., *et al.* (2013) Ground Water and Climate Change. *Nature Climate Change*, **3**, 322-329. <https://doi.org/10.1038/nclimate1744>
- [2] Cuthbert, M.O., Taylor, R.G., Favreau, G., Todd, M.C., Shamsudduha, M., Villholth, K.G., *et al.* (2019) Observed Controls on Resilience of Groundwater to Climate Variability in Sub-Saharan Africa. *Nature*, **572**, 230-234. <https://doi.org/10.1038/s41586-019-1441-7>
- [3] British Geological Survey (2018) Africa Groundwater Atlas.
- [4] MacDonald, A.M., Bonsor, H.C., Dochartaigh, B.É.Ó. and Taylor, R.G. (2012) Quantitative Maps of Groundwater Resources in Africa. *Environmental Research Letters*, **7**, Article ID: 024009. <https://doi.org/10.1088/1748-9326/7/2/024009>
- [5] Scanlon, B.R., Healy, R.W. and Cook, P.G. (2002) Choosing Appropriate Techniques for Quantifying Groundwater Recharge. *Hydrogeology Journal*, **10**, 18-39. <https://doi.org/10.1007/s10040-001-0176-2>
- [6] World Bank (2020) Kenya Water Security and Climate Resilience.
- [7] Funk, C., Paeterson, P., Landsfeld, M., Pedreros, D., Verdin, J., Shukla, S., *et al.* (2015) The Climate Hazards Infrared Precipitation with Stations—A New Environmental Record for Monitoring Extremes. *Scientific Data*, **2**, Article No. 150066. <https://doi.org/10.1038/sdata.2015.66>
- [8] Owor, M., Taylor, R.G., Tindimugaya, C. and Mwesigwa, D. (2009) Rainfall Intensity and Groundwater Recharge: Empirical Evidence from the Upper Nile Basin. *Environmental Research Letters*, **4**, Article ID: 035009. <https://doi.org/10.1088/1748-9326/4/3/035009>
- [9] Gates, J.B., Scanlon, B.R., Mu, X. and Zhang, L. (2011) Impacts of Soil Conservation on Groundwater Recharge in the Semi-Arid Loess Plateau, China. *Hydrogeology Journal*, **19**, 865-875. <https://doi.org/10.1007/s10040-011-0716-3>
- [10] Malczewski, J. (2006) Gis-based Multicriteria Decision Analysis: A Survey of the Lit-

- erature. *International Journal of Geographical Information Science*, **20**, 703-726. <https://doi.org/10.1080/13658810600661508>
- [11] Rodell, M., Famiglietti, J.S., Chen, J., Seneviratne, S.I., Viterbo, P., Holl, S., *et al.* (2004) Basin Scale Estimates of Evapotranspiration Using GRACE and Other Observations. *Geophysical Research Letters*, **31**, L20504. <https://doi.org/10.1029/2004gl020873>
- [12] Wiese, D.N., Landerer, F.W. and Watkins, M.M. (2016) Quantifying and Reducing Leakage Errors in the JPL RL05M GRACE Mascon Solution. *Water Resources Research*, **52**, 7490-7502. <https://doi.org/10.1002/2016wr019344>
- [13] Borzì, I., Bonaccorso, B. and Aronica, G.T. (2020) The Role of DEM Resolution and Evapotranspiration Assessment in Modeling Groundwater Resources Estimation: A Case Study in Sicily. *Water*, **12**, Article 2980. <https://doi.org/10.3390/w12112980>
- [14] Rodell, M., Velicogna, I. and Famiglietti, J.S. (2009) Satellite-Based Estimates of Groundwater Depletion in India. *Nature*, **460**, 999-1002. <https://doi.org/10.1038/nature08238>
- [15] Mann, H.B. (1945) Nonparametric Tests against Trend. *Econometrica*, **13**, 245-259. <https://doi.org/10.2307/1907187>
- [16] Sen, P.K. (1968) Estimates of the Regression Coefficient Based on Kendall's Tau. *Journal of the American Statistical Association*, **63**, 1379-1389. <https://doi.org/10.1080/01621459.1968.10480934>
- [17] Ferreira, V.G., Yang, H., Ndehedehe, C., Wang, H., Ge, Y., Xu, J., *et al.* (2024) Estimating Groundwater Recharge across Africa during 2003-2023 Using Grace-Derived Groundwater Storage Changes. *Journal of Hydrology: Regional Studies*, **56**, Article ID: 102046. <https://doi.org/10.1016/j.ejrh.2024.102046>
- [18] Leblanc, M.J., Favreau, G., Massuel, S., Tweed, S.O., Loireau, M. and Cappelaere, B. (2008) Land Clearance and Hydrological Change in the Sahel: SW Niger. *Global and Planetary Change*, **61**, 135-150. <https://doi.org/10.1016/j.gloplacha.2007.08.011>